IJBPAS, November, Special Issue, 2021, 10(11): 117-137
ISSN: 2277–4998

International Journal of Biology, Pharmacy and Allied Sciences (IJBPAS)
'A Bridge Between Laboratory and Reader'

www.ijbpas.com

DESIGN, SYNTHESIS, CHARACTERIZATION, AND BIOLOGICAL ACTIVITY OF SOME TRANSITION METAL COMPLEXES VIA NOVEL MANNICH BASE LIGAND

K. GOVINDARAJAN AND M. RAMESH*

Research Department of chemistry, Nehru Memorial College (Autonomous), (Affiliated to Bharathidasan University), Puthanampatti - 621007, Tamil Nadu, South India

***Corresponding Author: M. Ramesh; E Mail: drrameshnmc@gmail.com**

Received 19th July 2021; Revised 20th Aug. 2021; Accepted 29th Sept. 2021; Available online 1st Nov. 2021

https://doi.org/10.31032/IJBPAS/2021/10.11.1010

ABSTRACT

From the mannich base 2-((2,6-dioxocyclohexyl) (2-hydroxyphenyl) methyl) hydrazine carboxamide (**1**), a series of metal(II) complexes (**1a-1e**) ML with M = Cu(II), Ni(II), Fe(II), Cr(II), and Mn(II) were prepared and studied by electronic, IR, and NMR (^{1}H & ^{13}C) spectra, and molar conductivity measurements. The complexes are nonelectrolytes, according to conductivity measurements. All complexes have octahedral geometry, according to spectroscopy and other analytical investigations. The disc diffusion technique was used to test the antibacterial activity of ligand (**1**) and metal complexes (**1a-1e**) against *Staphylococcus aureus*, *Escherichia coli*, *Klebsiella pneumaniae*, and *Pseudomonas aeruginosa*. The metal complexes (**1a-1e**) were more effective than the control **Ciprofloxacin**.

Keywords: Mannich base, Transition metal complexes, Antibacterial activity, *Staphylococcus aureus*

INTRODUCTION

An acidic proton adjacent to a carbonyl group is amino alkylated with formaldehyde and ammonia or any primary or secondary amine in the Mannich reaction. A β-amino carbonyl molecule is the end result. Mannich reactions have also been proposed for

reactions involving imides and aromatic aldehydes. A survey of the literature on Mannich reactions reveals a large volume on the chemical, pharmacological, and toxicological characteristics of Mannich bases **[1-6]**, which have many uses as polymers, lubricant dispersants, and medicinal substances. Compounds with an amide moiety as a functional group were discovered to have donor characteristics and to have a broad variety of biological functions **[7-13]**. Transition metals are necessary for the proper functioning of living beings and also have a lot of promise as medicines **[14]**.

Owing to the sensitivity and selectivity of the ligands against different metal ions, metal complexes of Mannich bases were widely investigated in recent years **[15-19]**. Mannich process, to our understanding, is a three-component condensation process involving an active hydrogen-containing molecule, formaldehyde, and a secondary amine **[20]**. Extraction of solid complexes of various aromatic aldehydes or ketones, semicarbazones using transition metals has been studied extensively **[21, 22]**. There has been no research on the condensation of 1,3-cyclohexanedione, salicylaldehyde, and semicarbazide, according to the literature. The ability of semicarbazide compounds that contain the amide moiety to produce metal complexes is extensively documented in the literature. As a result, it was believed that synthesizing some metal complexes of this kind of Mannich base and investigating its bonding properties would be interesting. The three-component condensation of active hydrogen on 1,3-cyclohexanedione, salicylaldehyde, and semicarbazide yields 2-((2,6-dioxocyclohexyl) (2-hydroxyphenyl) methyl) hydrazine carboxamide (**1**), which we describe here. Monocoordination occurs in this ligand system owing to the O atom of semicarbazide.

Experimental

Chemicals and reagents

Merck and Sigma-Aldrich provided all of the chemicals, which were utilized without additional cleanup. The solvents have been purified and distilled before use. Merck's pre-coated silica gel plates with a fluorescent indication were utilized for analytical TLC. Silica gel chromatography of the flash column (Merck). The eluting solvent for TLC and column chromatography was ethyl acetate-hexane. Melting points were recorded in open capillary tubes and were not adjusted. The UV-Visible spectrum was obtained using a Shimadzu UV - 1280 (200-800 nm) spectrophotometer. The FT-IR

spectra (KBr) are obtained using a Shimadzu 8201pc (4000-400 cm-1) spectrophotometer.

Synthesis of Ligand (1)

In a 100mL RB flask, 1,3-cyclohexanedione (5.60 g, 0.05 mol), salicylaldehyde (6.1 mL, 0.05 mol), and Semicarbazide (0.05 mol, 5.57 g) were dissolved in 20mL ethanol. The contents of the flask are thoroughly stirred after 30 minutes of heating using a magnetic stirrer. After then, a brilliant crimson residue appeared. It has been dried and filtered. To produce pure product, the final prepared sample was recrystallized in hot ethanol. In **Scheme 1**, the production of ligand 1 is shown.

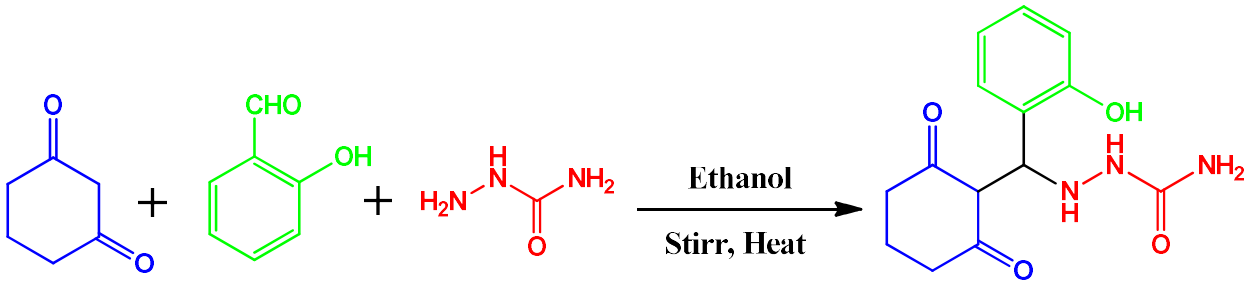

Scheme. 1. Synthesis of ligand 1

4.2.1.1. 2-((2,6-dioxocyclohexyl)(2-hydroxyphenyl) methyl) hydrazine carboxamide (1)

Red solid; mw: 291.30; mp:184°C; IR (KBr cm^{-1}) ν_{max}: 3435.94 (-OH), 2950.12 (-NH), 1638.73 (-C=O), 1237.44 (-C-N-C); ^1H NMR ($CDCl_3$, 300 MHz) δ 8.08 (s, 1H, NH), 7.12-6.90 (m, 4H, Ph-OH), 6.81 (d, *J* = 1.4 Hz ,1H, NH), 6.25 (s, 2H,NH_2), 5.64 (s, 1H, OH), 5.32 (d, *J* = 1.7 Hz, 1H, CH-Ph), 4.34 (d, *J* = 6.9 Hz, 1H, CHD), 2.47-1.95 (m, 6H, CHD); ^{13}C NMR ($CDCl_3$, 300 MHz) δ 208.83 (2C, C=O), 157.43 (1C, C=O), 154.01 (1C, C-OH), 130.19, 128.12, 126.56, 121.18, 115.72 (5C, Ar ring), 69.81 (1C, CH), 45.61 (1C, CH), 40.85 (2C, CH_2), 16.57 (1C, CH_2); EI-MS: m/z 292.13 (M^+,15%); Elemental analysis: Anal. Calcd. for $C_{14}H_{17}N_3O_4$: C, 57.72; H, 5.88; N, 14.42;%. Found: C, 57.70; H, 5.84; N, 14.48;%.

Synthesis of metal complexes (1a-1e)

Under continuous stirring, ligand **1** of hot ethanolic solution of (2 equivalent, 0.02 mol) was progressively combined with a metal chlorides in hot ethanolic solution (1 equivalent, 0.01 mol) under reflux. After refluxing for 1-2 hours, the mixture was chilled and stored in the refrigerator for a few hours. In each instance, the colored solid complexes were separated. It was filtered before being rinsed with 50% alcohol and dried.

Antibacterial activity

Antibacterial assessments of the ligand (**1**) and its complexes (**1a-1e**) were experienced in vitro against the bacteria *Staphylococcus aureus*, *Escherichia coli*, *Klebsiella pneumaniae*, and *Pseudomonas aeruginosa* by Kirby Bauer Disc diffusion method [23]. The antibacterial activity of ciprofloxacin was utilized as a reference. The bacterial cultures were cultivated on petri dishes on nutrient agar medium. The compounds were synthesized in DMSO and immersed in a 5 mm diameter, 1 mm thick filter paper disc. After 24 hours, the width of the inhibitory zone [24,25] surrounding each disc was evaluated for antibacterial activity, and the discs were put on the already implanted plates and incubated at 37°C. Minimum inhibitory concentrations (MIC) were used to reflect the antibacterial activity of ligand (**1**) and its metal complexes (**1a-1e**).

Results and discussion

Metal complexes (1a-1e) with ligand (1)

Physical data

Table 1 shows the physical belongings of the complexes (**1a-1e**) generated from ligand (**1**).

Solubility

The solubility of the ligand (**1**) and its associated complexes (**1a-1e**) in various solvents was investigated, and the findings are shown in **Table 2**. The ligand (**1**) as well as the metal complexes (**1a-1e**) soluble more readily in aprotic solvents than in protic solvents, according to solubility experiments.

Conductivity measurements

Numerous solvents, including water, ethanol, chloroform, and DMSO, were used to test the solubility of the newly synthesized metal complexes. The Equiptronics digital conductivity meter (Model EQ-660) was used to determine molar conductance in DMSO, with the cell constant calibrated using 0.1M KCl solution. The electrical conductivity of a 10^{-3} M solution of respective complexes in DMSO were determined, revealing the complexes' neutral (non-electrolytic) character. The molar conductance of the mixed ligand complexes (**1a-1e**) of ligand (**1**) ranges from 18 to 28 $\Omega^{-1}mol^{-1}cm^2$. The chloride ions were shown to be coupled to metal ions via conductivity tests, suggesting that they function as ligands rather than ions. Components for the produced complexes were selected depending on the metal – ligand ratios (1:2) and the type of the electrolytes as determined by conductance experiments, which aids in determining the structure of the complexes. The conductance properties of metal complexes (**1a-1e**) with ligand (**1**) were shown in **Table 3**.

NMR Spectral studies of ligand (1)

The hydrogens of the aromatic rings show a multiplet at 7.12-6.90 ppm in the ^{1}H NMR spectrum of the Mannich base ligand (**1**) below investigation **(Figure 1)**. The methylene hydrogens linked to the salicylaldehyde and amine hydrogens of the semicarbazide show as a peak at 4.34 ppm, whereas the aromatic –OH occurs at 5.64 ppm. The absence of an indication equivalent to the secondary amine $–NH_2$ proton as it was removed in the Mannich process further confirms the creation of the ligand. The carbons of the aromatic rings had peaks at 130.19-115.72 ppm in the ^{13}C NMR spectra of the Mannich base ligand (**1**) under investigation **(Figure 2)**. The presence of a peak at 45.61 ppm shows that the methylene carbon is linked to the semicarbazide's salicylaldehyde and amine hydrogens, respectively. Furthermore, the carbonyl carbons of the 1,3-cyclohexanedione and semicarbazide moiety are represented by the peaks at 208.83 and 157.43 ppm, accordingly.

IR Spectra

The existence of a strong band at 3435.94 and 1638.73cm^{-1}, which is attributed to vOH and the C=O carbonyl group, is a significant finding in the ligand spectrum (Fig. 3). The bands attributable to C=O and O-H moved towards lower frequency in all of the complexes (Fig. 4-8), suggesting that carbonyl oxygen and hydroxyl oxygen were engaged in coordination through metal ions. In copper complex (**1a**), the M-O bond is represented by the new peak appeared at 757.42 cm^{-1}. The M-Cl bond is represented by the new peak at 526.68 cm^{-1}. The IR Spectral data of the complexes (**1a-1e**) and the ligand (**1**) were displayed in **Table 4**.

UV-Visible Spectra

The ligand and complex UV-visible spectra were obtained in the region of 100-1100 nm. The UV spectra of ligand (1) primarily revealed two strong maximum bands at 380nm and 525nm, which correspond to the $\pi \rightarrow \pi^*$ and $n \rightarrow \pi^*$ transitions, respectfully **(Figure 9)**. The octahedral geometry of the Cu (II) complex being investigation is suggested by a wide band in the 300nm range. The octahedral structure of the Ni (II) complex was confirmed by wide peaks at 263nm and 311nm. The octahedral structure of the bands found for Cr (II) complex also displays wide peaks at 263nm and 301nm. Broad signals were seen at 263nm and 321nm for the Fe (II) complex, confirming its octahedral shape. The Mn (II) complex emitted wide signals at 262 nm, indicating that it is octahedral. **Figure 10-14** shows the UV spectrums of metal complexes (**1a-1e**).

EPR spectra

The type of metal ligand bond formation along with the dispersion of paired and unpaired electrons may be learned through EPR spectrum analysis. Cu (II) complexes have a unique character in coordination chemistry, with geometries such as tetrahedral, square planar, octahedral, and square pyramidal that may be distinguished by EPR spectrometry. $g\parallel$, $g\perp$, gavg and G are EPR parameters that indicate if the compound is octahedral or tetrahedral. The following criterion confirms the existence of an unpaired electron in the dx^2-y^2 orbital: $g\parallel > g\perp > 2.0023$. For the copper complex, the measured $g\parallel$ and $g\perp$ values are 2.1581 and 2.0138, correspondingly. The ionic nature is shown by a $g\parallel$ value more than 2.3, while the covalent nature is indicated by a $g\parallel$ value less than 2.3. We can see that the $g\parallel$ value (2.1581) is smaller than 2.3, indicating that the compound is covalent. According to Hathaway, G values less than four indicate a significant exchange contact between metal centers, whereas G values higher than four indicate a minimal charge transfer. The G value is 4.76 in this case, thus the exchange interaction is insignificant. The Cu (II) complex exhibits deformed octahedral geometry, according to the EPR characteristics. The EPR spectra of copper complex (**1a**) was shown in **Figure 15**.

Suggested Structure of the Complexes

We propose the following structure of complexes produced with the Mannich base ligand based on the preceding findings.

Biological screening

Antibacterial activity

The antibacterial activity of the synthesized ligand (**1**) and complexes (**1a-1e**) were tested. The ligand (**1**) had low activity compared to the corresponding complexes (**1a-1e**). The investigation was done in a controlled environment. In the (**1a-1e**), series, the complex **1a** was only highly active, with an MIC value of 2 µg/mL in *S.aureus*. Obviously, the chromium complex **1d** was more active against *K.neumoniae*, with MIC value of 4 µg/mL, than the control **Ciprofloxacin**, which had MIC value of 8 µg/mL. The iron complex **1c** was more active against *E.coli*, with MIC value of 4 µg/mL, than the control **Ciprofloxacin**, which had MIC value of 6 µg/mL. In comparison to complexes (**1a-1e**), complex **1a** (Cu II), complex **1c** (Fe II), and complex **1d** (Cr II), has exceptional activity. **Table 5** summarizes the findings.

Table 1: Physical data of the complexes (1a-1e) and ligand (1)

Compound	Colour	Melting point (^{o}C)
Ligand (1)	Red	184
Copper complex (1a)	Blue	210
Nickel complex (1b)	Pale green	214
Iron complex (1c)	Brown	226
Chromium complex (1d)	Green	208
Manganese complex (1e)	White	220

Table 2: Solubility test results

Compound	Water	Ethanol	Chloroform	DMSO
Ligand (1)	Insoluble	Insoluble	Sparingly soluble	Soluble
Copper complex (1a)	Insoluble	Insoluble	Insoluble	Soluble
Nickel complex (1b)	Insoluble	Insoluble	Insoluble	Soluble
Iron complex (1c)	Insoluble	Insoluble	Insoluble	Soluble
Chromium complex (1d)	Insoluble	Insoluble	Insoluble	Soluble
Manganese complex (1e)	Insoluble	Insoluble	Insoluble	Soluble

Table 3: Conductance properties of metal complexes (1a-1e) with ligand (1)

S. No	Compounds	Conductance ($\Omega^{-1}mol^{-1}cm^{2}$)
1.	Copper complex (1a)	18
2.	Nickel complex (1b)	28
3.	Iron complex (1c)	24
4.	Chromium complex (1d)	22
5.	Manganese complex (1e)	23

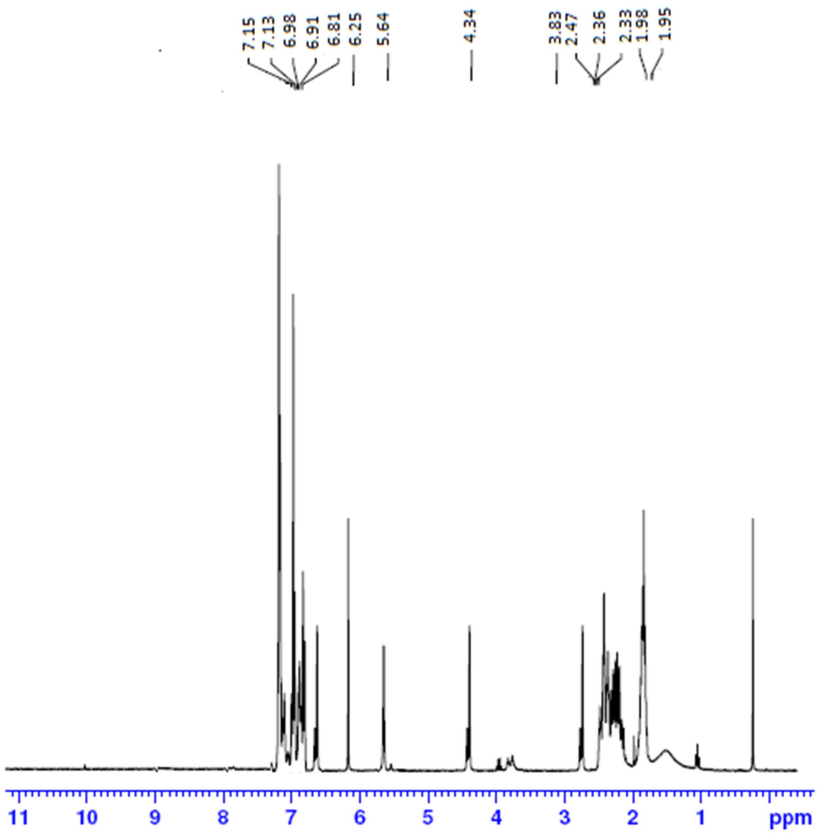

Figure 1: Ligand (1)-^{1}H-NMR spectra

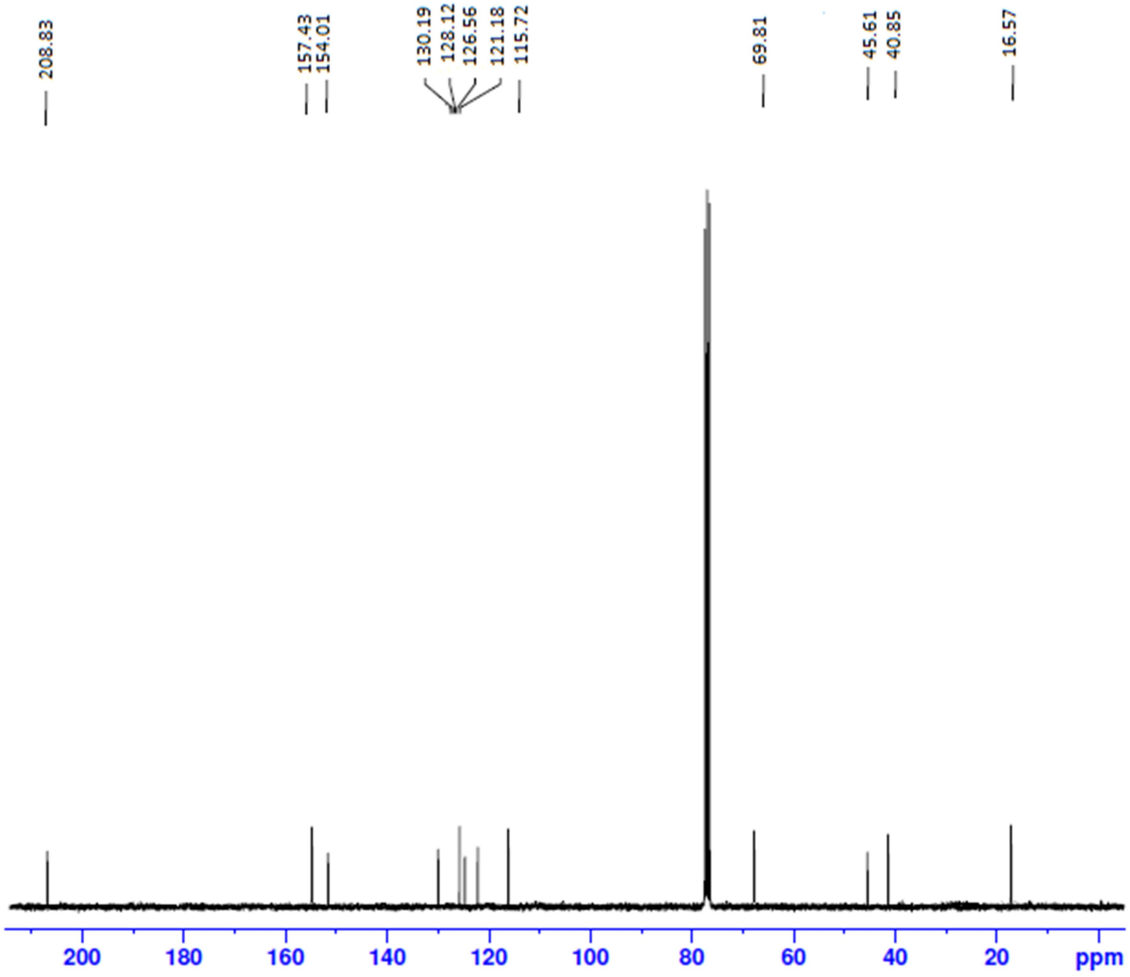

Figure 2: Ligand (1)-^{13}C-NMR spectra

Table 4: IR Spectral data of the complexes (1a-1e) and the ligand (1)

	IR stretching frequency (cm^{-1})			
Compound	**-OH**	**-C=O**	**M-O**	**M-Cl**
Ligand (1)	**3435.94**	**1638.73**	**-**	**-**
Copper complex (1a)	**3392.75**	**1633.69**	**757.42**	**526.68**
Nickel complex (1b)	**3465.32**	**1624.01**	**755.22**	**546.16**
Iron complex (1c)	**3416.11**	**1640.87**	**758.19**	**525.93**
Chromium complex (1d)	**3431.63**	**1633.14**	**757.24**	**525.14**
Manganese complex (1e)	**3437.60**	**1642.27**	**757.74**	**525.25**

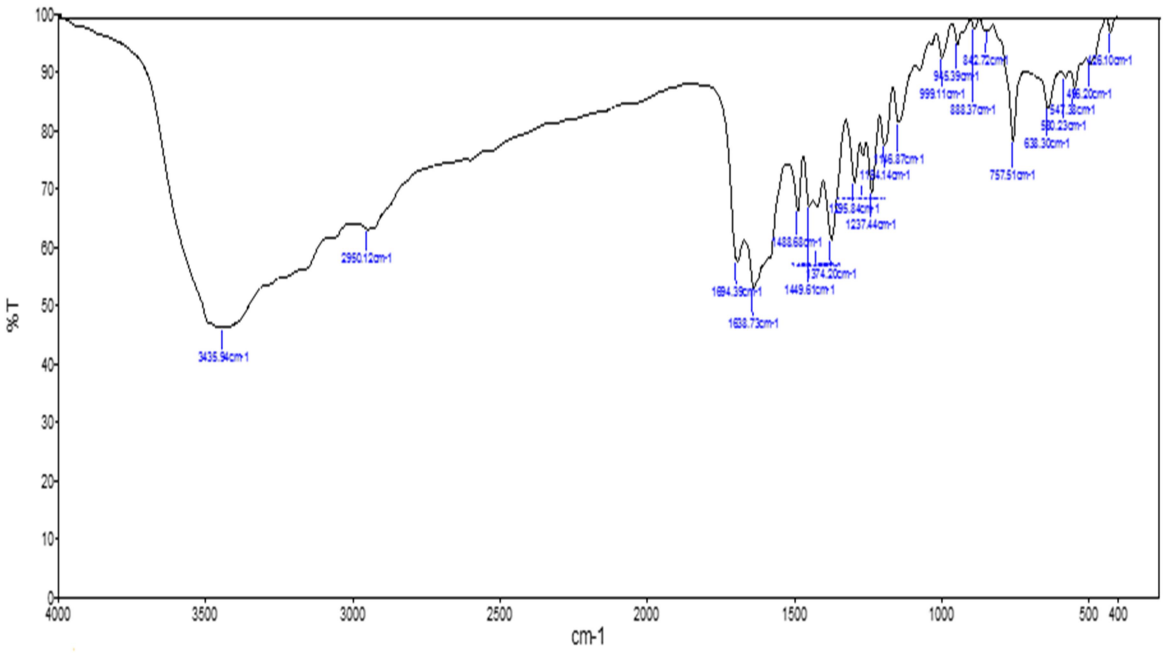

Figure 3: Ligand (1) FT-IR spectra

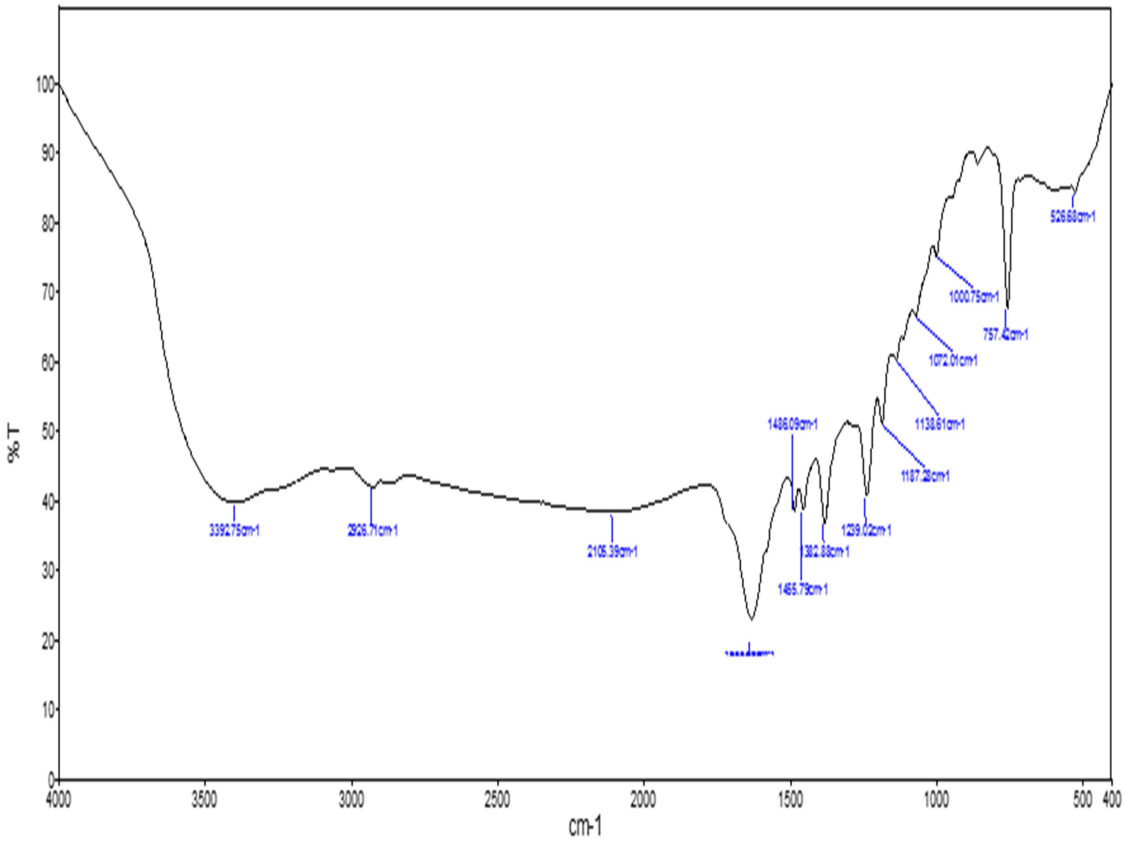

Figure 4: Copper complex (1a) FT-IR spectra

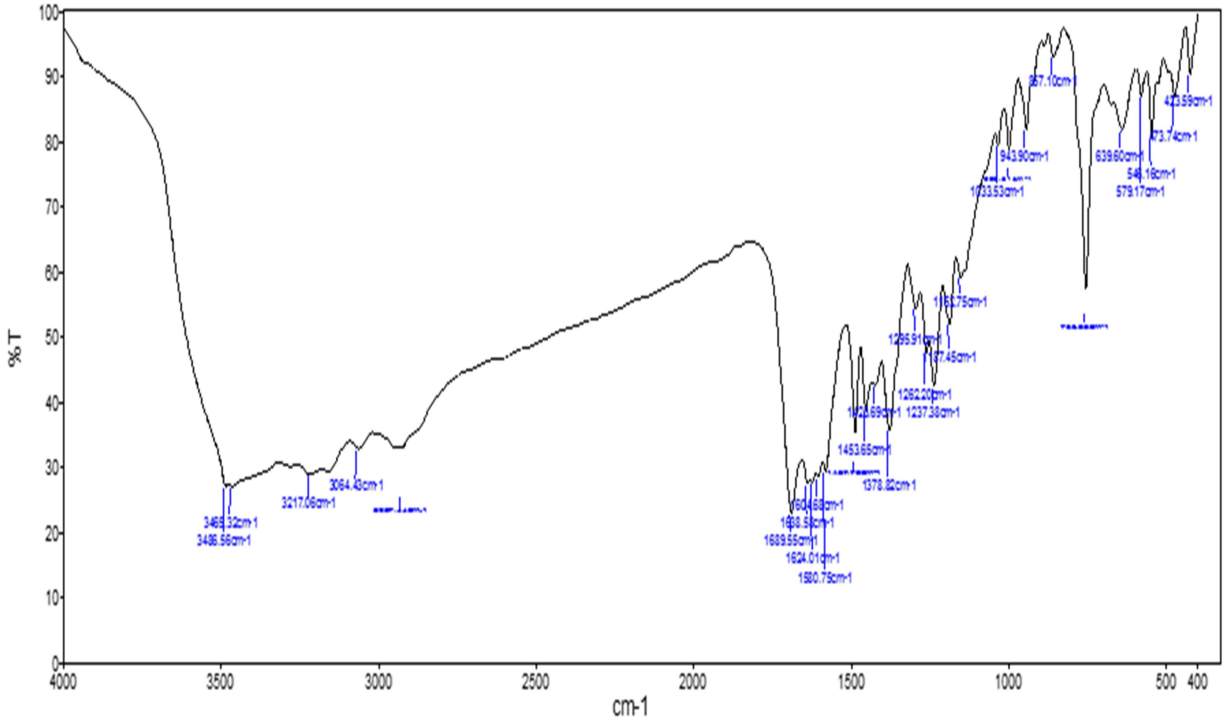

Figure 5: Nickel complex (1b) FT-IR spectra

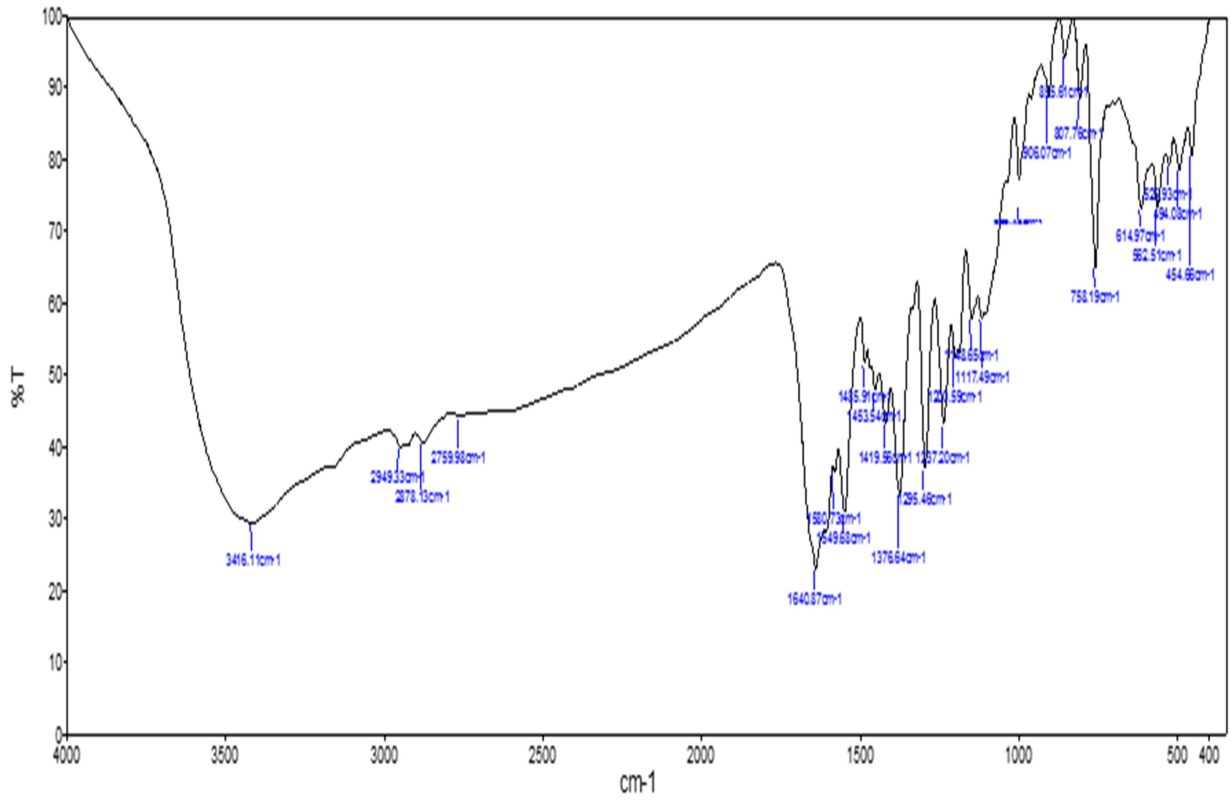

Figure 6: Iron complex (1c) FT-IR spectra

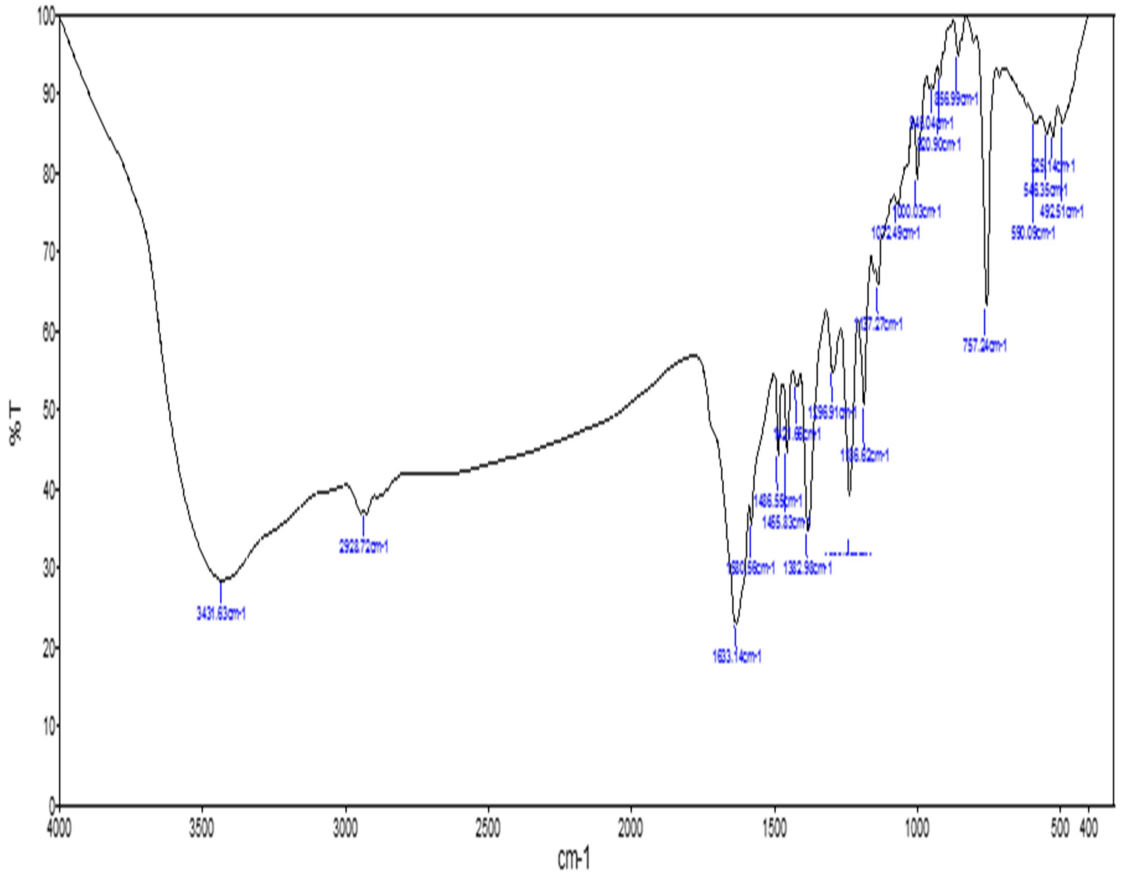

Figure 7: Chromium complex (1d) FT-IR spectra

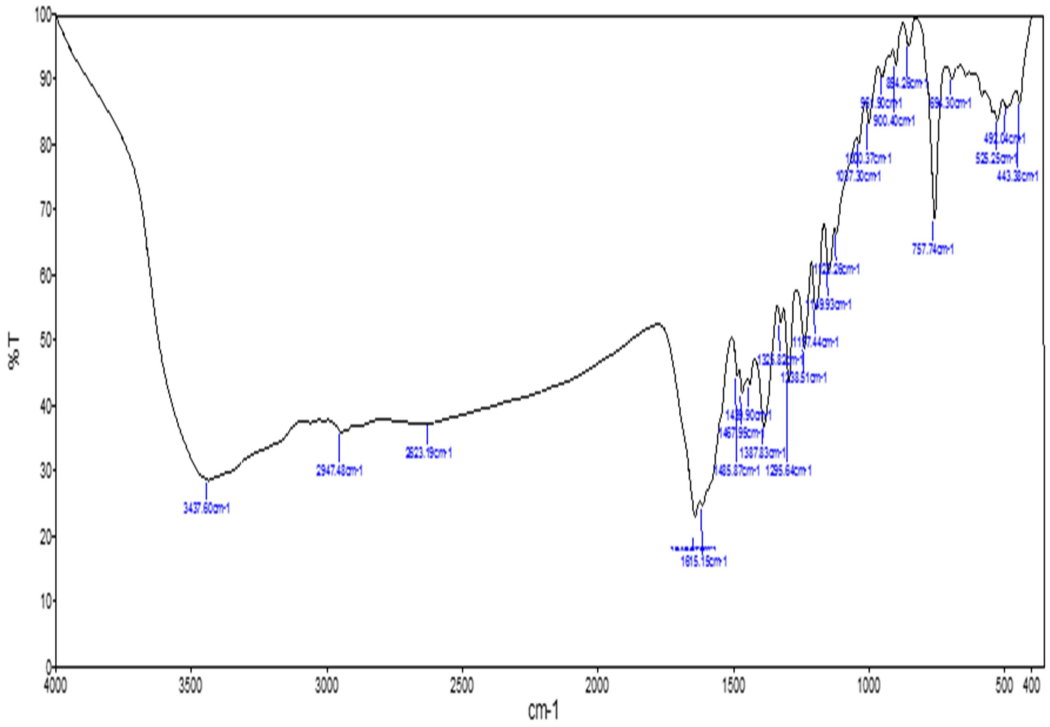

Figure 8: Manganese complex (1e) FT-IR spectra

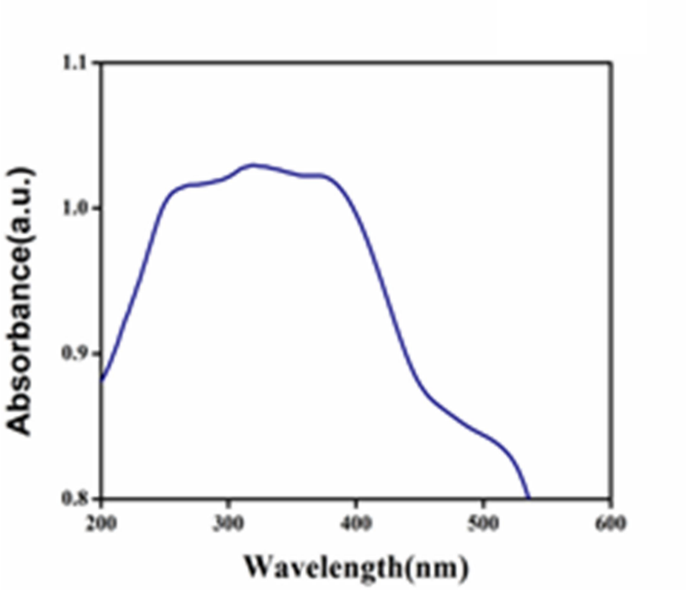

Figure 9: Ligand 1 UV-spectra

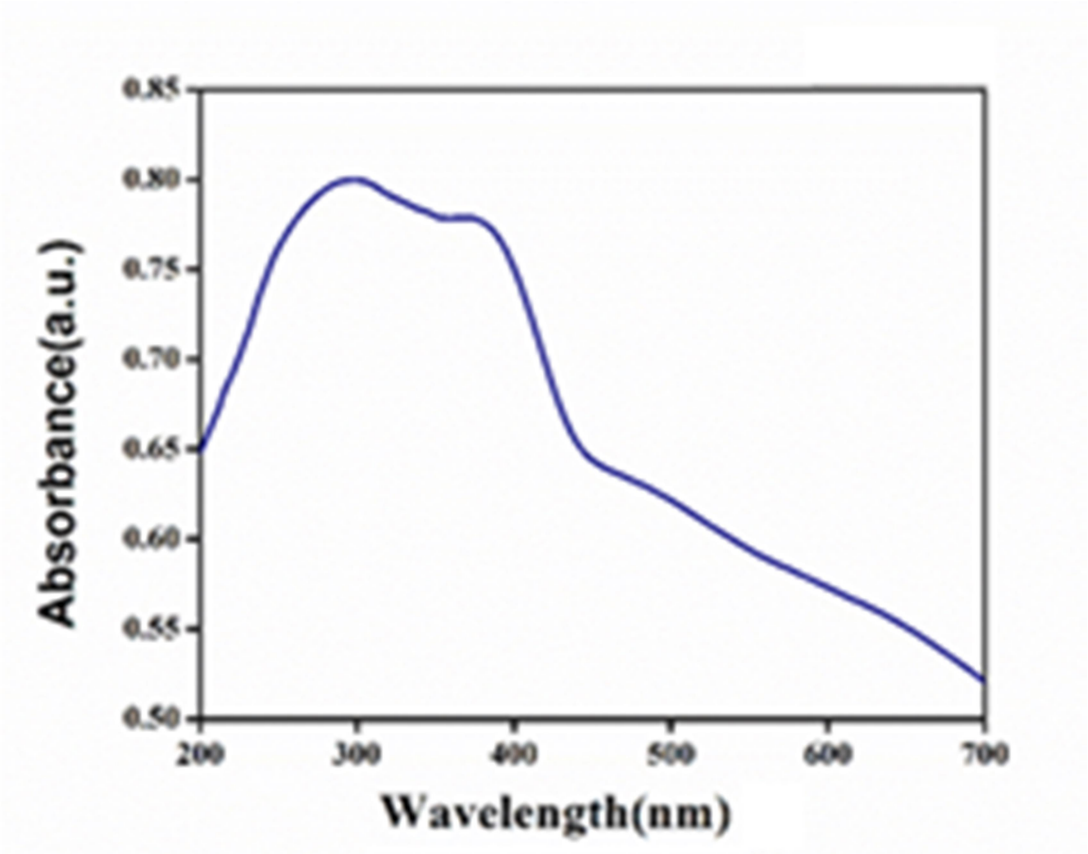

Figure 10: Copper complex (1a) UV-Spectra

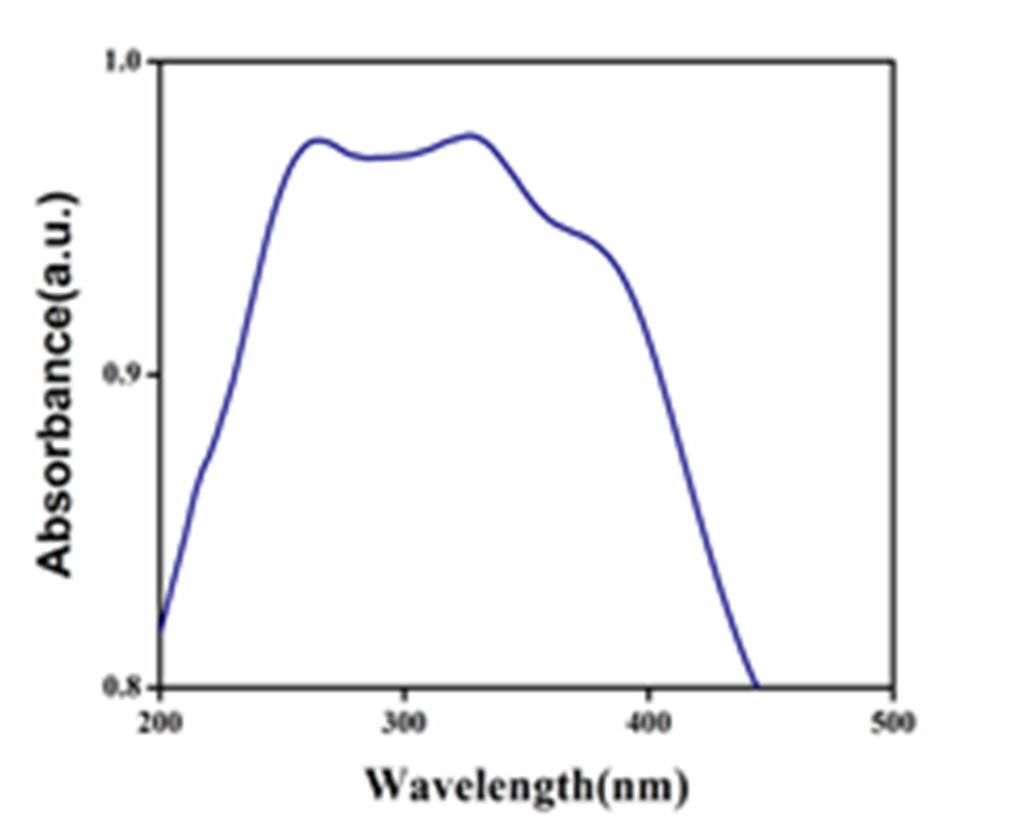

Figure 11: Nickel complex (1b) UV-Spectra

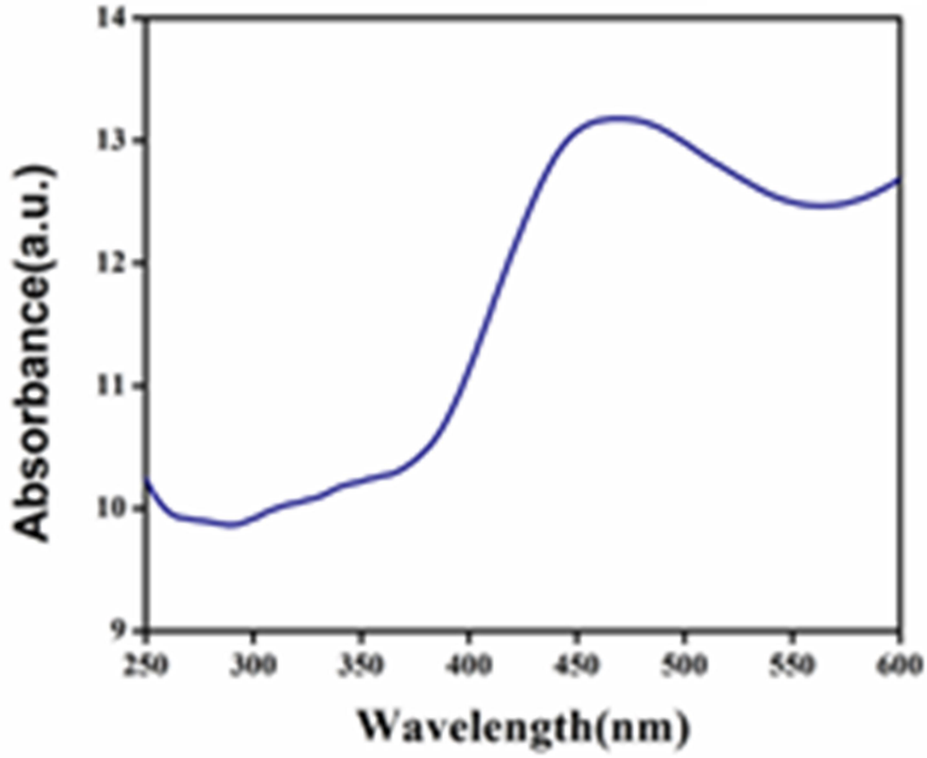

Figure 12: Iron complex (1c) UV-Spectra

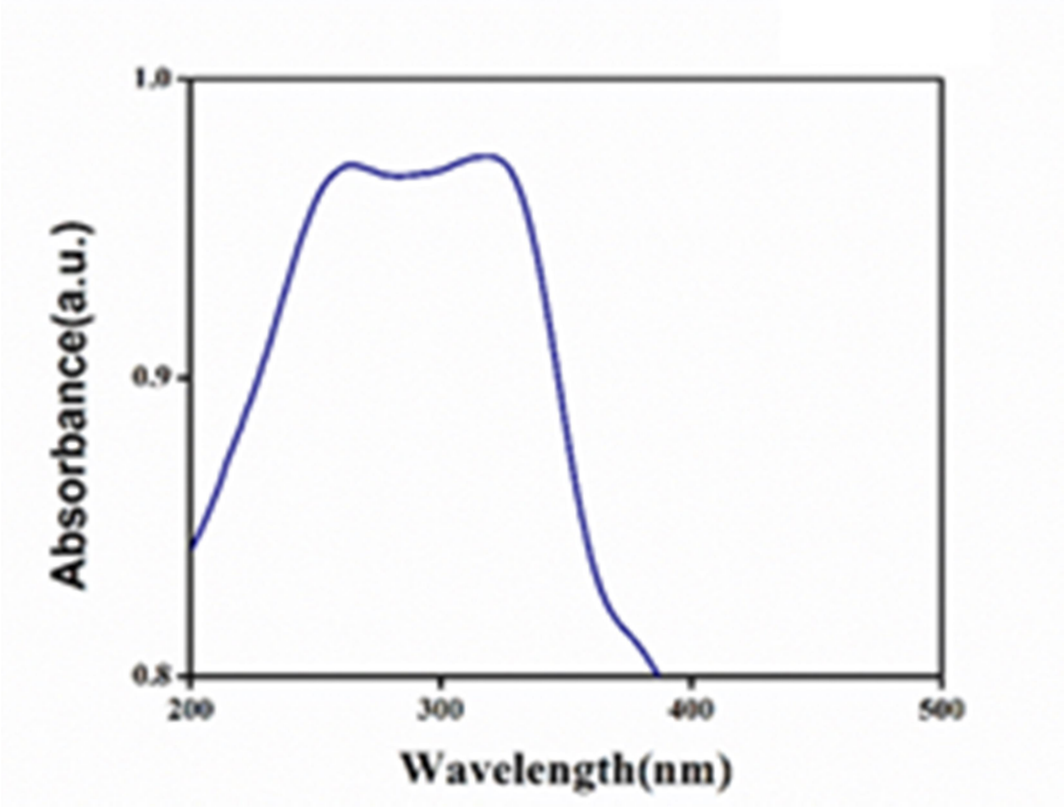

Figure 13: Chromium complex (1d) UV-Spectra

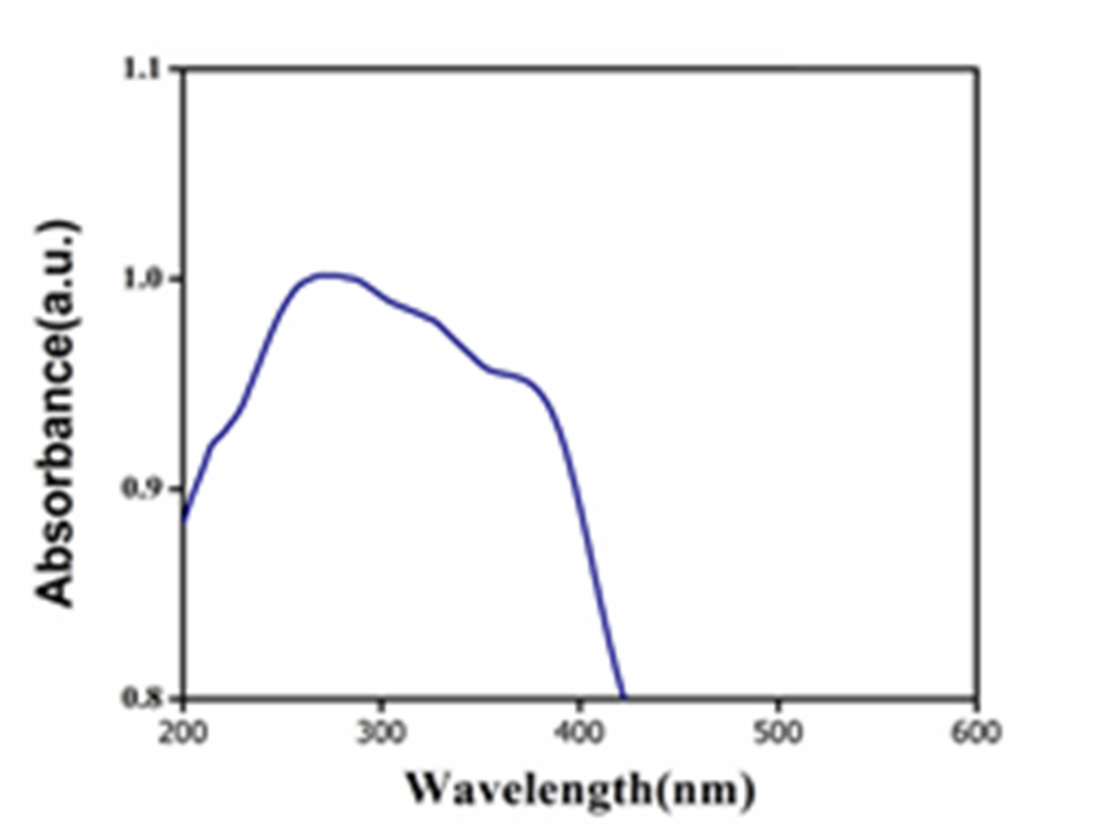

Figure 14: Manganese complex (1e) UV-Spectra

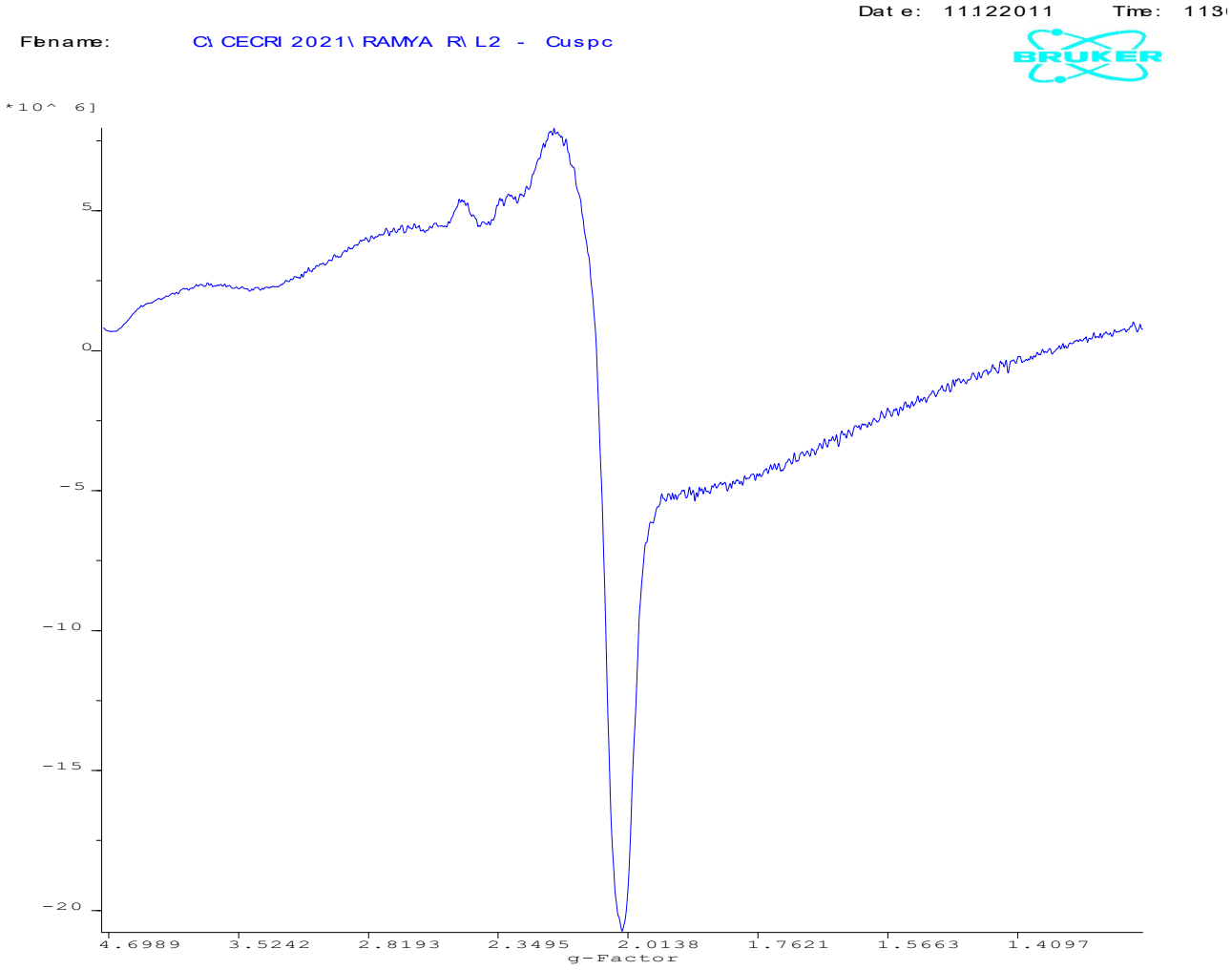

Figure 15: Copper complex (1a) EPR spectra

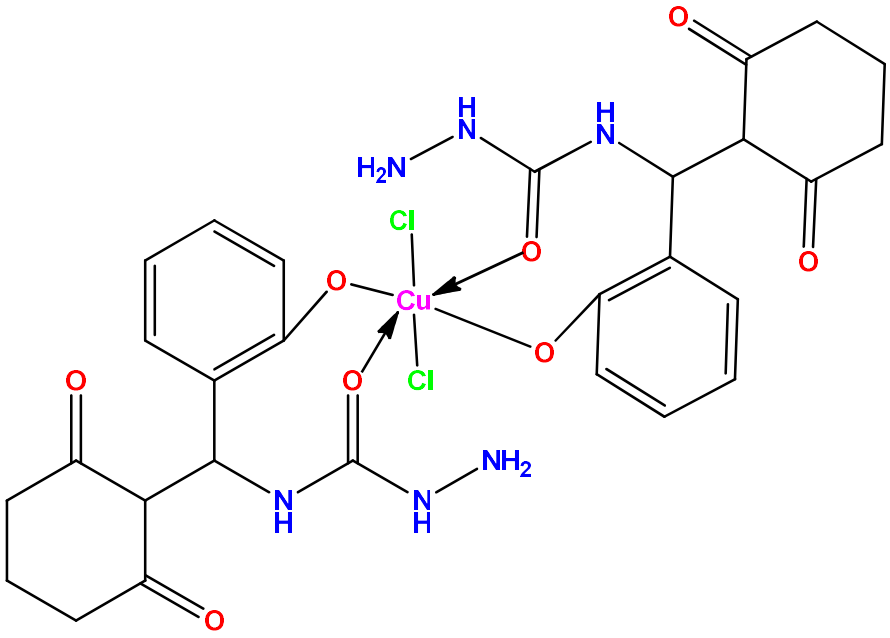

Structure of the Copper complex (1a) with ligand 1

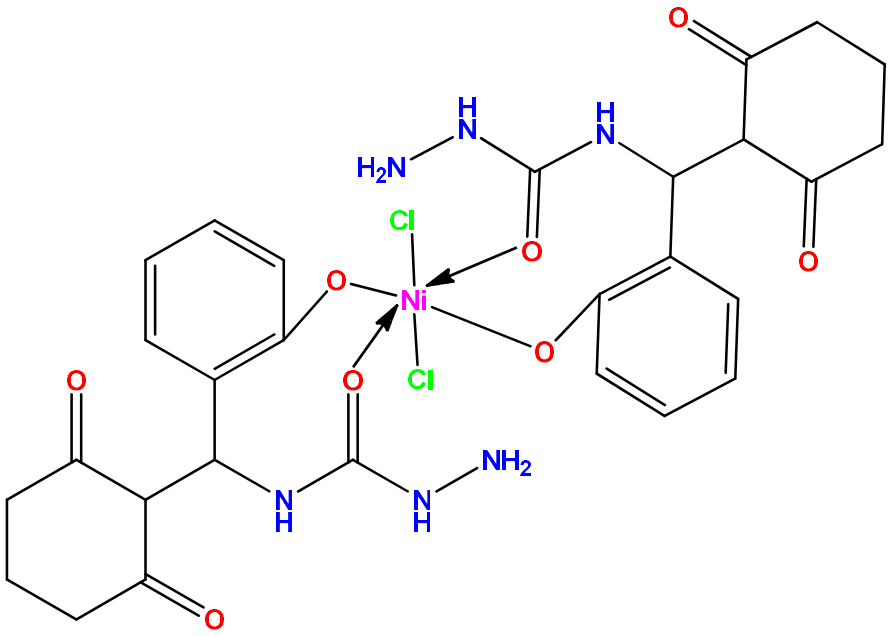

Structure of the Nickel complex (1b) with ligand 1

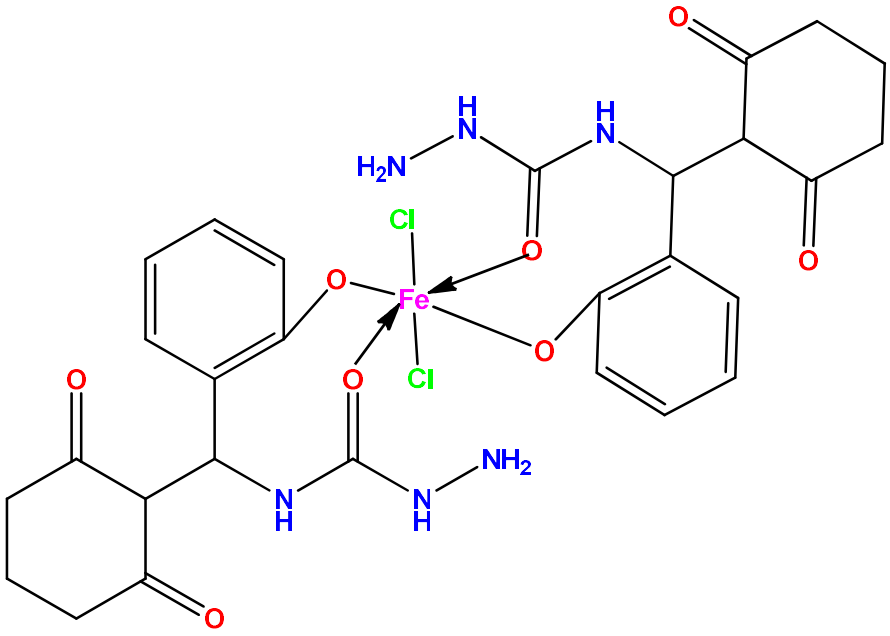

Structure of the Iron complex (1c) with ligand 1

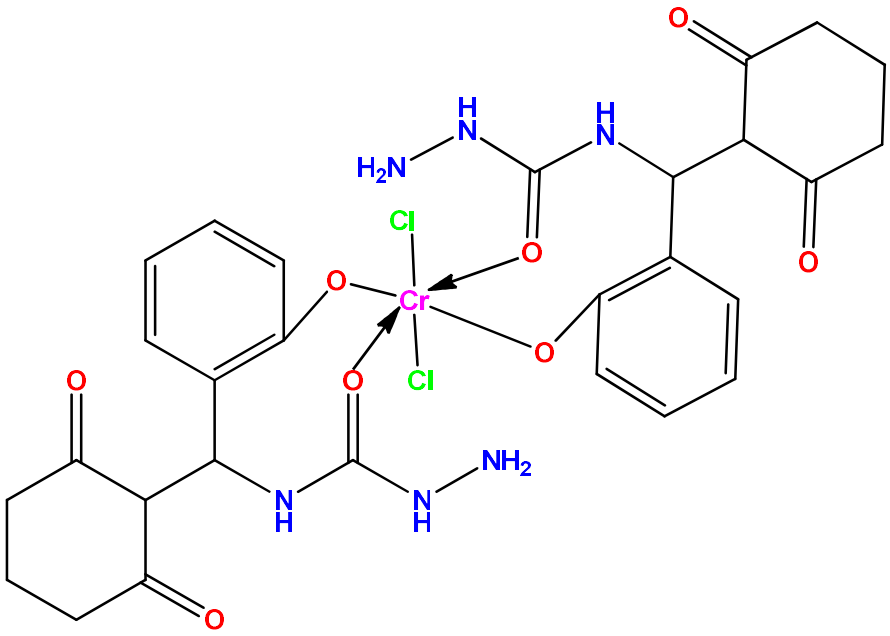

Structure of the Chromium complex (1d) with ligand 1

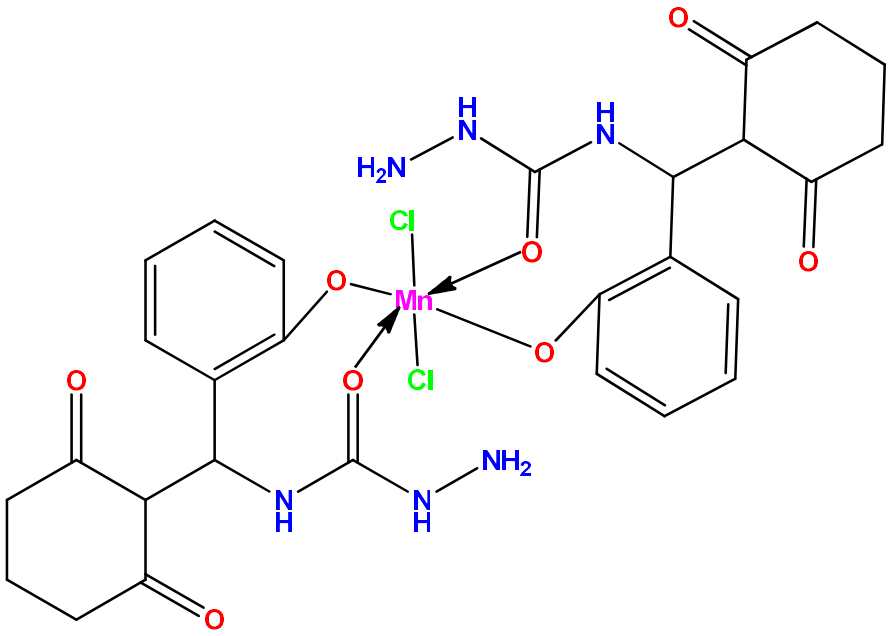

Structure of the Manganese complex (1e) with ligand 1

Table 5: Antibacterial assessment of ligand (1) and its complexes (1a-1e)

Compounds	Minimum inhibitory concentration (MIC) in µg/mL			
	S. aureus	*K. pneumaniae*	*E. coli*	*P. aeruginosa*
1	32	16	16	32
1a	2	12	10	8
1b	8	28	8	8
1c	10	14	4	4
1d	6	4	12	4
1e	12	16	8	4
Ciprofloxacin	4	8	6	2

CONCLUSION

The coordination behavior of a Mannich base ligand synthesized from 1,3-cyclohexanedione, salicylaldehyde, and semicarbazide is reported in this article. Using the aforementioned Mannich base ligand, Cu (II), Ni (II), Fe (II), Cr (II), and Mn (II) complexes were produced and described using analytical and spectroscopic techniques. The Mannich base functions as a neutral bidentate ligand by coordinating to the metal ion via its semicarbazide oxygen and salicylaldehyde oxygen. The complexes are all octahedral in shape. The ligand (**1**) as well as its metal complexes (**1a-1e**) have been found to have considerable antibacterial action against several disease causing bacterial strains. Over **ciprofloxacin**, the metal complexes proved to be an effective bactericide.

Acknowledgments

K. Govindarajan acknowledges Assistant Professor, DR. M. Ramesh of Nehru Memorial College, Tiruchirapalli,

TamilNadu for his constant support for this research.

Conflicts of interest

The authors declare no conflicts of interest.

REFERENCES

[1] Tramontini, Maurilio. "Advances in the chemistry of Mannich bases." Synthesis 1973, no. 12 (1973): 703-775.

[2] Tramontini, Maurilio, and Luigi Angiolini. "Further advances in the chemistry of Mannich bases." Tetrahedron 46, no. 6 (1990): 1791-1837.

[3] Tramontini, Maurilio, and Luigi Angiolini. Mannich bases-chemistry and uses. Vol. 5. CRC Press, 1994.

[4] Joshi, Sheela, Navita Khosla, and Prapti Tiwari. "In vitro study of some medicinally important Mannich bases derived from antitubercular agent." Bioorganic & medicinal chemistry 12, no. 3 (2004): 571-576.

[5] Manikpuri, A. D., S. Joshi, and P. V. Khalidkar. "synthesis and antimicrobial study of the mannich bases of4-{(dipropylamino)[bis (methylene)] sulfanyl} benzamide." Journal of Engineering Science and Management Education 2 (2010): 29-33.

[6] Joshi, S., N. Khosla, D. Khare, and P. Tiwari. "Synthesis and antibacterial screening of novel sulphonamide Mannich bases." ACTA PHARMACEUTICA-ZAGREB- 52, no. 3 (2002): 197-206.

[7] Raman, N., and S. Ravichandran. "Synthesis and characterization of a new Schiff base and its metal complexes derived from the Mannich base, N-(1-piperidinobenzyl) acetamide." Synthesis and Reactivity in Inorganic, Metal-Organic, and Nano-Metal Chemistry 35, no. 6 (2005): 439-444.

[8] Borisova, N. E., Yu A. Ustynyuk, M. D. Reshetova, G. G. Aleksandrov, I. L. Eremenko, and I. I. Moiseev. "Binuclear and polynuclear transition metal complexes with macrocyclic ligands. 5. Novel complexes of asymmetric polydentate macrocyclic Schiff bases. Step-by-step synthesis." Russian chemical bulletin 53, no. 2 (2004): 340-345.

[9] Bokam, Y. K., Guntupalli, C., Gudhanti, S. N. K. R., Manne, R., Alavala, R. R., & Alla, N. R. (2021). Importance of pharmacists as a front line warrior in improving medication compliance in Covid 19 patients. Indian Journal of Pharmaceutical Sciences, 83(2), 398-401.

[10] Gangadasu, B., P. Narender, B. Raju, and V. Jayathirtha Rao. "Calcium chloride catalyzed three

component, one-pot condensation reaction: An efficient synthesis of 3, 4-dihydropyrimidin-2 (1H)-ones." (2006).

[11] Braide, W., S. U. Oranusi, and C. C. Otali. "Microbiological status of processed fruit juice sold in the commercial city of Onitsha." Scholarly Journal of Biological Science 1, no. 3 (2012): 25-30.

[12] Carta, Fabrizio, Andrea Scozzafava, and Claudiu T. Supuran. "Sulfonamides: a patent review (2008–2012)." Expert opinion on therapeutic patents 22, no. 7 (2012): 747-758.

[13] Walsh, Christopher. "Enabling the chemistry of life." Nature 409, no. 6817 (2001): 226-231.

[14] Malhotra, Ekta, N. K. Kaushik, and H. S. Malhotra. "Synthesis and studies of ionic chelates of hafnocene with guanine." (2006).

[15] Cossins, Dan. "Archive for the 'Medication'Category." Schizophr Bull 38, no. 5 (2012): 911-913.

[16] Cleare, M. J. "Transition metal complexes in cancer chemotherapy." Coordination Chemistry Reviews 12, no. 4 (1974): 349-405.

[17] Singh, B., R. N. Singh, and R. C. Aggarwal. "Magnetic and spectral studies on N-(thiophene-2-carboxamido) salicylaldimine complexes of some bivalent 3d metal ions." Polyhedron 4, no. 3 (1985): 401-407.

[18] Sodha, Mahendra Singh, Shikha Misra, S. K. Mishra, and Sweta Srivastava. "Growth of embryonic dust particles in a complex plasma." Journal of Applied Physics 107, no. 10 (2010): 103307.

[19] Ahmad, Sayeed, Sultan Zahiruddin, Bushra Parveen, Parakh Basist, Abida Parveen, Rabea Parveen, and Minhaj Ahmad. "Indian medicinal plants and formulations and their potential against COVID-19–preclinical and clinical research." Frontiers in pharmacology 11 (2021): 2470.

[20] Singh, Akshay K., Anjali Srivastava, Vivek Kumar, and Karunakar Singh. "Phytochemicals, medicinal and food applications of Shatavari (Asparagus racemosus): An updated review." The Natural Products Journal 8, no. 1 (2018): 32-44.

[21] Zhou, Z. A., Zhenghe Xu, J. A. Finch, J. H. Masliyah, and R. S. Chow. "On the role of cavitation in particle collection in flotation–A critical review. II." Minerals Engineering 22, no. 5 (2009): 419-433.

[22] Braide, W., R. N. Nwaoguikpe, S. U. Oranusi, L. I. Udegbunam, C.

Akobondu, and S. I. Okorondu. "The effect of biodeterioration on the nutritional composition and microbiology of an edible long-winged reproductive termite, Macroterms bellicosus. Smeathman." Internet Journal of Food Safety 13 (2011): 107-114.

[23] Mohanasundaram.S, VA Doss, Haripriya G, Varsha M, Daniya S, Madhankumar (2017). GC-MS analysis of bioactive compounds and comparative antibacterial potentials of aqueous, ethanolic and hydroethanolic extracts of Senna alata L against enteric pathogens. Int. J. Res. Pharm. Sci., 8 (1): 22 – 27.

[24] Victor Arokia Doss, Mohanasundaram.S, Prasad Maddisetty (2016). Analysis of hydroethanolic extract of Senna alata (L.) to screen bioactive compounds with inhibitory activity on lipid peroxidation, in vitro antibacterial and antidiabetic efficacy. Int J Pharma Sci., 6(1): 1360-1366.

[25] S. Narendhiran, S. Mohanasundaram, J. Arun, L. Saravanan, L. Catherine, M. Subathra, R.V. Rannjith, Prasanna, Alagesan, Buvaneshwri (2014). Comparative study in larvicidal efficacy of medicinal plant extracts against Culex quinquefasciatus. International Journal of Research in Plant Science; 4(1): 22-25.